IIETA International Information and Engineering Technology Association
Advancing the World of Information and Engineering

Revue des Composites et des Matériaux Avancés-Journal of Composite and Advanced Materials
Vol. 36, No. 4, August, 2026, pp. 929-936
Journal homepage: http://iieta.org/journals/rcma

Fabrication and Characterization of Conductive AuNPs-loaded PCL/PU Electrospun Scaffolds for Cardiac Tissue Engineering Potential

Saja A. Moosa*, Tiba Y. Jasim, Hadeel A. Abbas, Akram R. Jabur

College of Materials Engineering, University of Technology-Iraq, Baghdad 10066, Iraq

Corresponding Author Email: saja.a.moosa@uotechnology.edu.iq

https://doi.org/10.18280/rcma.360420

Received: 3 April 2026
Revised: 24 June 2026
Accepted: 6 July 2026
Available online: 31 August 2026

Keywords:
electrospinning, cardiac tissue engineering, nanofibrous scaffold, electrical conductivity, polycaprolactone/polyurethane blend, gold nanoparticles

ABSTRACT

Repairing heart tissue presents a major clinical challenge, driving the development of biomaterials that mimic the natural environment of the heart muscle. This study focuses on the fabrication and characterization of electrically conductive fibrous nanostructures using polycaprolactone (PCL) and polyurethane (PU), two materials commonly used in biomedical research. To improve electrical conductivity, we incorporated gold nanoparticles (AuNPs) within the scaffold matrix. We characterized the fabricated structures using scanning electron microscopy (SEM) and Fourier transform infrared spectroscopy (FTIR). The SEM results showed a homogeneous fibrous structure with diameters ranging from 499 to 853 nm. Furthermore, FTIR analysis showed physical interactions between the AuNPs and the polymer matrix without compromising structural integrity. The contact angle results demonstrated that the incorporation of AuNPs improved the hydrophilicity of the surface. It is worth noting that the addition of AuNPs significantly increased the electrical conductivity of the supporting structures. Based on our results, the physical, chemical, and electrical properties of PCL:PU-AuNPs composite scaffolds make them suitable for cardiac tissue engineering applications. Further studies such as cell adhesion and in vitro cytotoxicity testing need to be performed in order to validate the biological performance of these scaffolds for cardiac regeneration.

1. INTRODUCTION

Globally, cardiovascular diseases (CVDs) represent the major cause of mortality, causing about 18 million deaths yearly, with ischemic heart disease being the most prevalent [1, 2].

The available methods of treatment, including heart transplantation, have serious shortcomings such as the unavailability of donors, immune rejection, and cost. Accordingly, cardiac tissue engineering has been proposed as a strategy to regenerate damaged myocardial tissue using bioengineered scaffolds that can replicate the native extracellular matrix (ECM) [3-5]. The manufacture of nanofibrous scaffolds has received significant interest via electrospinning technology because of its ability to mimic the natural ECM structure.

Such materials offer controlled porosity, large surface-area-to-volume ratios, and requisite mechanical characteristics for cell adhesion and proliferation [6, 7]. Polycaprolactone (PCL) is a well-known biodegradable polymer with good processability, but due to its hydrophobic property, cellular interactions can be limited [8, 9]. Polyurethane (PU), on the other hand, has better elasticity and wettability, thus being applicable in soft tissue applications [10].

Mechanical strength and flexibility can be merged by combining PCL and PU [11-13]. However, the two polymers are electrically insulating, and this limits their usage in the regeneration of electrically active cardiac tissues. Electrical conductivity is essential to cardiomyocytes' coordination [14]. In order to solve this problem, researchers have introduced polyaniline and carbon nanotubes (CNTs) in scaffolds.

However, their cytotoxicity, lack of biodegradability, and complex production methods pose significant challenges [15-17]. A promising alternative is gold nanoparticles (AuNPs), which offer high biocompatibility, electrical conductivity, and easy synthesis and can be biologically functionalized [18, 19]. Recent studies show AuNPs enhance electrical properties and support cell growth in tissue engineering scaffolds [20, 21]. This work aims to develop and characterize electrospun PCL:PU scaffolds decorated with AuNPs, evaluating their structural, morphological, and electrical properties for cardiac tissue engineering.

2. MATERIALS AND METHODS

2.1 Materials

We purchased medical-grade PU molecular weight (Mw) = 150,000 Daltons (Da) and PCL Mw = 80,000 Da) from Sigma-

Aldrich. We sourced Dichloromethane (DCM) and N,N-dimethylformamide (DMF) from Central Drug House (P) and Alpha Chemika, respectively. We obtained spherical AuNPs (average size 20–30 nm, 99.95% purity) from Hongwu International Group Ltd. We used all substances without further purification.

2.2 Electrospinning solutions preparation

We dissolved both PCL and PU separately in a 9:1 (v/v) mixture of DCM and DMF to obtain 10% (w/v) solutions, then magnetically stirred the mixture for 5 hours at a speed of 75 rpm. Next, we mixed PCL and PU in a specific weight ratio and magnetically stirred the mixture for five hours to obtain a homogeneous solution. Finally, we prepared the gold nanoparticle-loaded mixture by adding 1 wt.% AuNPs to the PCL:PU solution and stirring the mixture for one hour in an ultrasonic homogenizer to ensure homogeneous dispersion.

2.3 Electrospinning process

We used a horizontal electrospinning machine. We filled a 10 mL syringe fitted with a 22-gauge needle with the polymer solution. We set the parameters at a flow rate of 1 mL/h, a voltage of 18 kV, and a distance between the probe tip and the collector of 15 cm. We collected the scaffolds on an aluminum-wrapped drum collector and vacuum-dried all samples for 24 hours to remove any remaining solvents.

2.4 Characterization techniques

2.4.1 Scanning electron microscopy analysis

The morphology and diameter of the fiber were examined under a VEGA3 LM-TESCAN scanning electron microscope. The samples were sputtered with gold, and images were taken at 10 kV. The average fiber diameter and pore size were calculated using ImageJ and OriginPro software.

2.4.2 Energy dispersive X-ray spectroscopy

Energy dispersive X-ray spectroscopy (EDS) analysis was conducted to characterize the elemental composition of the scaffolds.

2.4.3 Fourier transform infrared spectroscopy

The chemical composition was analyzed by a BRUKER TENSOR-27 infrared spectrometer in the spectral region 4000-400 cm^{-1}.

2.4.4 Electrical conductivity

Electrical resistance was measured by the 2-point probe method using a KEITHLEY 616 digital electrometer. Electrical conductivity was calculated from the standard resistivity equation. Three measurements were taken on each scaffold to ensure data reliability and to determine the surface homogeneity. Final electrical conductivity was calculated as the average of three measurements ± standard deviation.

2.4.5 Water contact angle

The wettability was evaluated using a CAM 110 goniometer. A 5 µL drop of distilled water was dropped onto each sample, and measurements were taken at three different locations.

2.4.6 Atomic force microscopy

The surface topography and roughness of the nanofibrous scaffolds have been examined using atomic force microscopy (AFM) in tapping mode.

3. RESULTS AND DISCUSSION

This section presents and discusses results of electrospun scaffolds focusing on key analyses: morphological features, fiber diameter and pore size distributions, FTIR spectroscopy, electrical conductivity, and surface wettability. These properties are crucial in determining the suitability of these scaffolds for cardiac tissue engineering.

3.1 Morphology and microstructure/energy dispersive X-ray spectroscopy

Scanning electron microscopy (SEM) analysis was carried out to determine the morphology of the scaffold, diameter of the fibers, and the size of the pores (Figures 1-4).

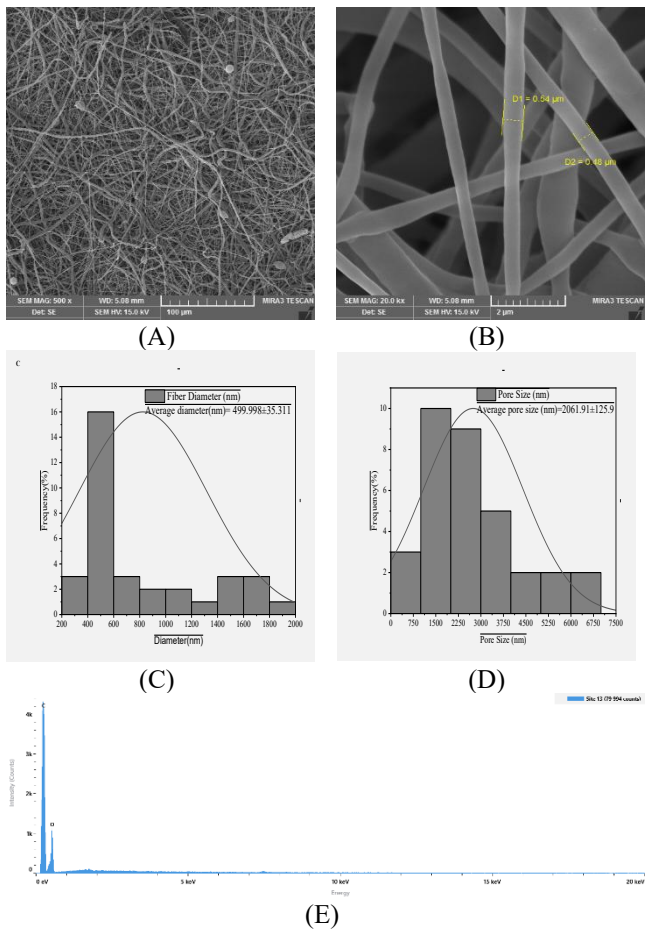

Figure 1. (A) Scanning electron microscopy (SEM) image of 10% w/v pure polycaprolactone (PCL) at 500X magnification; (B) SEM image at 20KX magnification; (C) mean fiber diameter; (D) mean pore size; (E) energy dispersive X-ray spectroscopy (EDS) spectrum

As shown in Figure 1(A-D), the average diameter and pore size of the pure PCL substrate were found to be 499.99 ± 35 nm and 2061.9 ± 125 nm, respectively, and fibers on this substrate were uniform without evidence of beads. They are dense fibres that can hamper cell infiltration. As shown in the

EDS spectrum in Figure 1(E), the spectrum exhibits two prominent peaks indicating carbon (C) and oxygen (O), the two fundamental constituents of the PCL polymer repeating units. The absence of additional impurity peaks confirms the high purity of the produced nanofibers and the efficiency of the electrospinning technique in maintaining their chemical homogeneity.

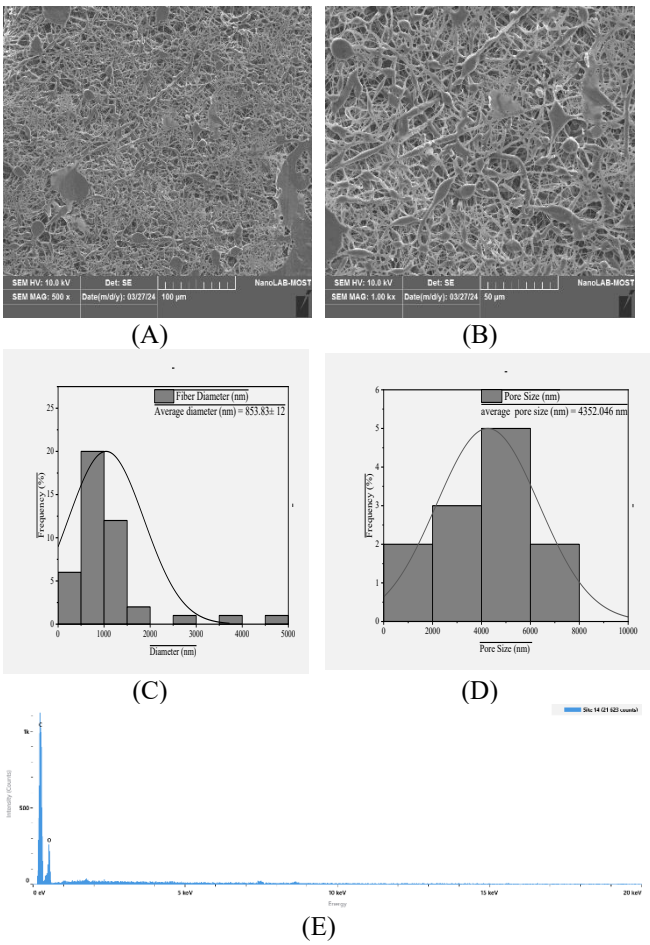

Figure 2. (A) Scanning electron microscopy (SEM) image of 10% w/v pure polyurethane (PU) at 500X magnification; (B) SEM image at 1KX magnification; (C) mean fiber diameter; (D) mean pore size; (E) energy dispersive X-ray spectroscopy (EDS) spectrum

In contrast, the pure PU scaffold (Figure 2) displayed a more open structure, with a larger fiber diameter of 853.83 ± 12 nm and a pore size of 4, 250.05 ± 589 nm, most likely due to the higher molecular weight and solution viscosity of PU. The PCL:PU blend (in a ratio of 3:1) (Figure 3) exhibited intermediate morphology (diameter: 811.5 nm; pore size: 4, 352.05 nm). We observed that the PCL:PU structure loaded with AuNPs (Figure 4) contained spherical nanoparticles uniformly decorated on the fiber surfaces. While these pores facilitate transport of nutrients, their range of 2 to 4 µm may limit the depth of cell infiltration, since the size of cells usually exceeds these dimensions. We recognize this as a limitation and suggest that improving parameters in the future could enhance pore interconnectivity. EDS spectrum of the gold-decorated PCL:PU nanofibers, presented in Figure 4. E confirms the successful incorporation of AuNPs into the polymer matrix. Despite the characteristic peaks of C and O, distinct peaks of Au are clearly seen. This result confirms the effectiveness of integrating and distributing AuNPs within nanofiber structures fabricated by the electrospinning process, demonstrating the robustness of the synthesis technique.

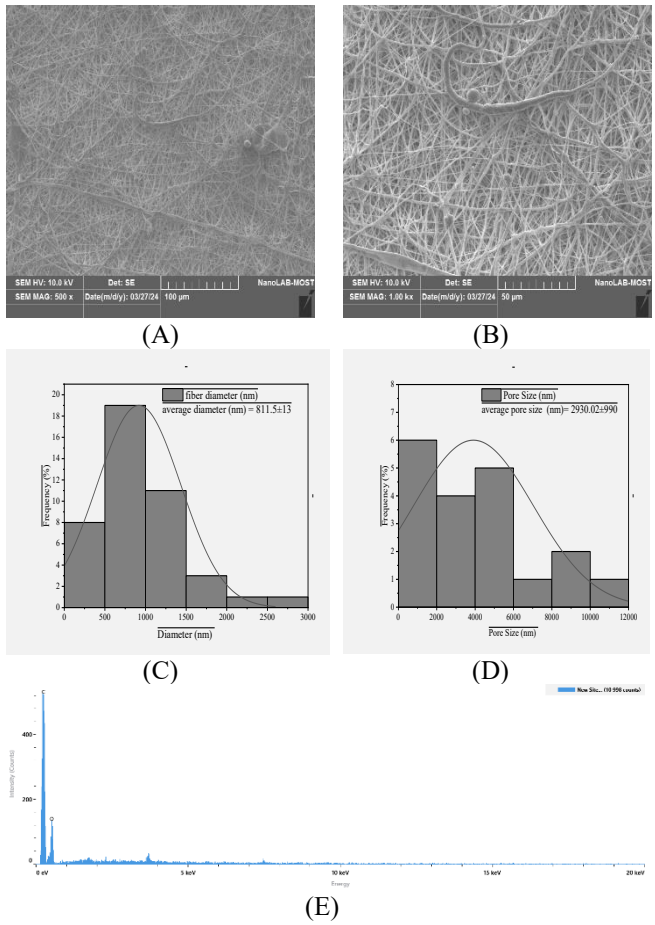

Figure 3. (A) Scanning electron microscopy (SEM) image of 10% w/v polycaprolactone (PCL): polyurethane (PU) (3:1) at 500X magnification; (B) SEM image at 20KX magnification; (C) mean fiber diameter; (D) mean pore size; (E) energy dispersive X-ray spectroscopy (EDS) spectrum

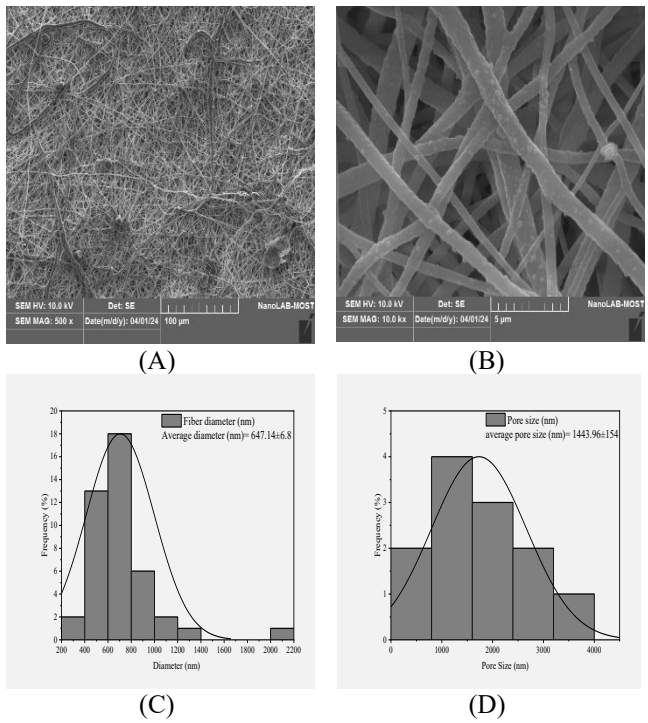

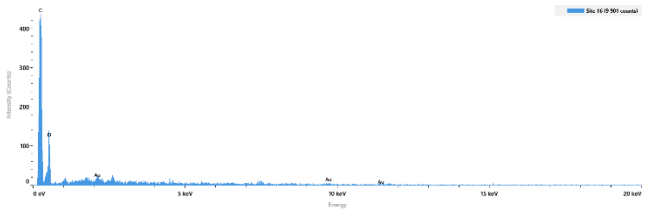

(E)

Figure 4. (A) Scanning electron microscopy (SEM) image of gold nanoparticles (AuNPs)- polycaprolactone (PCL): polyurethane (PU) at 500X magnification; (B) SEM image at 10KX magnification; (C) mean fiber diameter; (D) mean pore size; (E) energy dispersive X-ray spectroscopy (EDS) spectrum

3.2 Fourier transform infrared spectroscopy

We used FTIR analysis to evaluate the chemical composition and interactions within the scaffolds' structure (Figures 5 and 6). Pure PCL (Figure 5(A)) showed characteristic peaks at 1, 722.31 cm^{-1} (C=O stretching), 2, 943.14 cm^{-1} as well as 2, 865.4 cm^{-1} (C-H stretching), and 1, 045; 1, 106.61; and 1, 239 cm^{-1} (C-O-C stretching), consistent with literature values [15, 16, 18]. Pure PU (Figure 5(B)) exhibited a broad N-H bond stretching at 3328 cm^{-1}, C=O stretching at 1, 727 cm^{-1}, and aromatic C=C bond stretching at 1531 cm^{-1}. The sharp peak at 1, 221 cm^{-1} is attributed to the stretching C-O-C bond in the ester, a characteristic feature of urethane bonds in PU [17].

The PCL:PU blend (Figure 6(A)) exhibited an overlap of these peaks, indicating a physical blend without chemical bonds. Conversely, the spectrum of PCL:PU loaded with AuNPs (Figure 6(B)) revealed slight peak shifts and broadening. These shifts indicate weak physical interactions, such as electrostatic coordination between AuNPs and the polymer's functional groups, which we expect will improve the electrical performance of the composite.

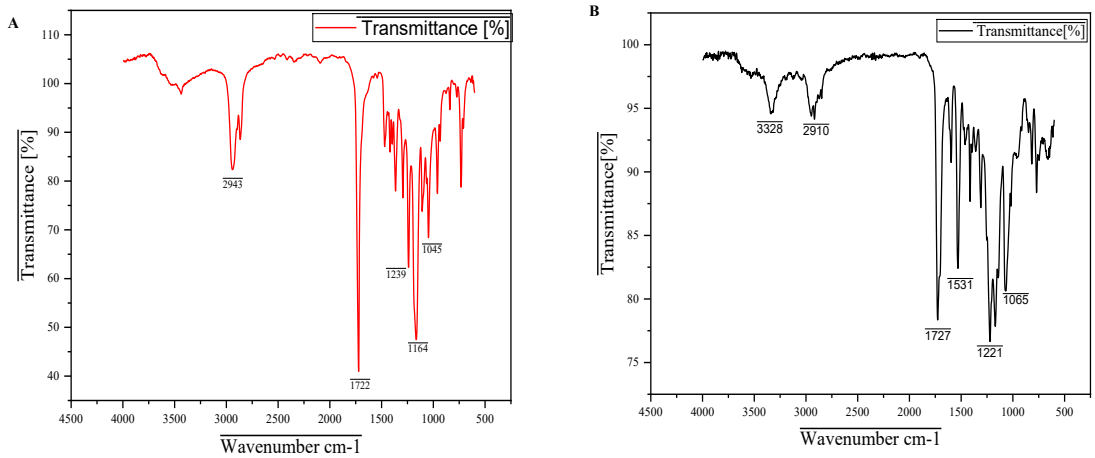

Figure 5. Fourier transform infrared spectroscopy (FTIR) spectra of nanofibrous scaffolds fabricated entirely from (A) polycaprolactone (PCL) polymer; (B) polyurethane (PU) polymers

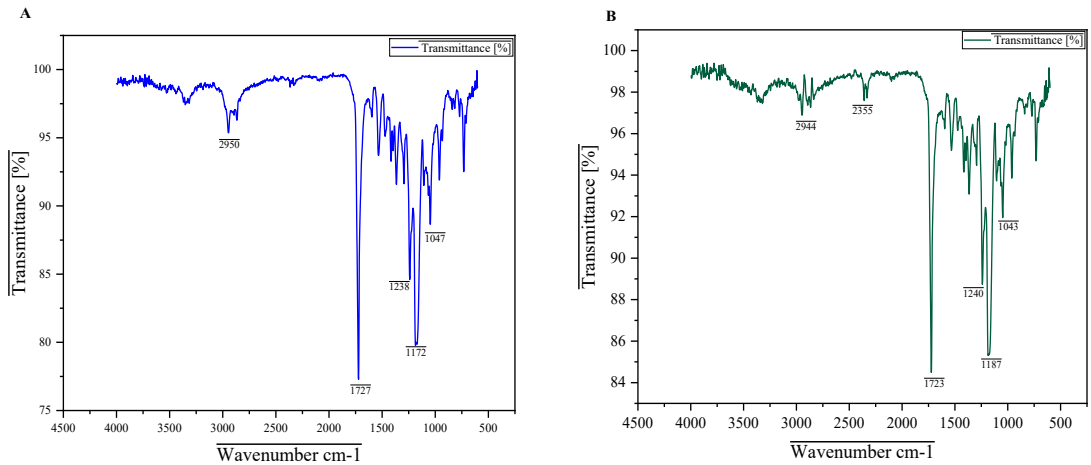

Figure 6. Fourier transform infrared spectroscopy (FTIR) spectra of nanofibrous scaffolds composed of (A) PCL:PU (3:1); (B) gold nanoparticles (AuNPs)- PCL:PU

Note: Polycaprolactone (PCL), polyurethane (PU).

3.3 Electrical conductivity

We calculated the electrical conductivity of the structures loaded with AuNPs-scaffolds using a standard resistivity formula with the two-point probe technique.

$$R = (\rho L)/(Wt) \quad (1)$$

$$\sigma = 1/\rho \quad (2)$$

where, ρ is resistivity, R is electrical resistance, and L, W, and

t represent length, width, and thickness, respectively, for mats [19]. As shown in Figure 7, the pure PCL structure acted as an electrical insulator, displaying a negligible electrical conductivity of 1.2×10^{-4} S/cm, which is insufficient for cardiac tissue engineering applications, where signal propagation is required. In contrast, we observed a significant increase in electrical conductivity, reaching 0.0352 S/cm in the PCL:PU blend. When AuNPs were incorporated, the conductivity reached 0.54 S/cm. SEM analysis reveals that the AuNPs are mainly distributed on the surface of the nanofibers, a phenomenon known as surface segregation. The shear force of the spinning action during electrospinning forces the nanoparticles to migrate to the outside of the fibers due to fast solvent evaporation. This surface distribution is very critical for creating a conductive network within the scaffold in 3D. Randomly oriented nanofibers that are gold-decorated congregate together at many points of contact when they meet. These junctions serve as electron-transporting pathways, enabling electron transfer within the scaffold. This network of interconnected nanoparticles at the interfaces between the fibers is thought to be the real reason for the measured conductivity, as the pure PCL:PU structure is by nature insulating, and this is achieved even with this relatively small filler loading.

To evaluate these results, we compared our findings with the values reported in the scientific literature for conductive polymer structures. Typically, the scaffolds of CNTs have an extremely high conductivity (from 1 to 5 S/cm), but are limited by their reactivity and inflammatory response within the body [20-24]. Our value of conductivity was 0.54 S/cm, which is reasonable as compared to other systems containing AuNPs and nanofibres (0.1–0.7 S/cm). This level of conductivity is appropriate for facilitating the electromechanical signals essential for synchronized cardiomyocyte contraction of cardiac muscle cells. Furthermore, our approach based on AuNPs offers a biocompatibility profile compared to carbon or metal-based alternatives, providing a balance between electrical performance and cellular safety.

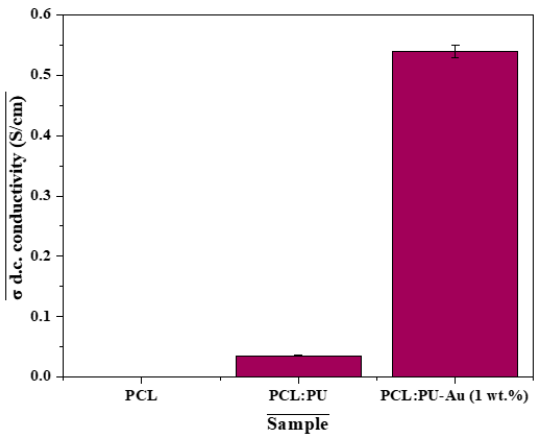

Figure 7. The Electrical conductivity of gold nanoparticles (AuNPs)-incorporated scaffolds produced through electrospinning

3.4 Wettability and surface properties

The wettability of the scaffold surface was assessed using a goniometer to study how scaffold composition affects surface energy. Pure PCL, due to its hydrophobic nature, exhibited a relatively high water contact angle (WCA) Figures 8 and 9. Conversely, we observed that the PCL:PU blend showed an improvement in hydrophilicity, which is attributed to the incorporation of the more hydrophilic PU component. When AuNPs were added, we observed a further increase in the surface's hydrophilicity. This improvement is most likely due to the high surface energy and polar functional groups of the AuNPs, which enhance the spreading of the water droplet. Although surface roughness (Ra) (as illustrated by Wenzel and Cassie-Baxter models [25]) inherently affects wettability, we attribute the observed hydrophilic property mainly to the chemical composition and the uniform distribution of AuNPs within the fiber network. This hydrophilic surface property is of great importance for future biological applications, as it normally facilitates better protein uptake and cell adhesion in cardiac tissue engineering [26-28].

3.5 Atomic force microscopy results

AFM analysis provided a detailed view of the surface topography of the PCL nanofibers. The two-dimensional (2D) and three-dimensional (3D) images (Figure 10(A)) revealed a uniform distribution of nanostructure properties along the fiber surface. The observed average Ra was 1.017 µm, and the root-mean-square roughness (Rq) was 1198.9 nm, while the Sq value reached 1272.7 nm, confirming the hierarchical, textured structure of the fiber surface. The surface characteristics are expected to achieve a better surface area, which could lead to better cell adherence and proliferation. Using AFM analysis, the Ra of the nanofibers of these PUs was found to be 1.035 µm (Figure 10(B)). PU structures exhibited slightly higher Ra than PCL structures, which may be attributed to inherent differences in polymer chain movement and electrospinning behavior. These recorded topographical parameters (such as Sq [1.513 µm]) were especially complex, potentially contributing to an increase in surface area, in diffusion of nutrients, and in cell-material interactions. When PCL was blended with PU, a unique surface morphology was obtained. AFM analysis (Figure 10(C)) showed a lower mean Ra of 555.6 nm, in comparison with each individual polymer scaffold, indicating that a better, more even blending process was conducted. The PCL fibers have a more even and uniform surface topography, which is probably due to the smoothing effect of the PU. Surface morphology was examined for the PCL:PU/Au samples, and it was observed that their surface was found to be much more refined (Ra = 261.99 nm) compared to the pure polymer PCL and PU counterparts. This reduction indicates that the properties of the AuNPs brought a smoothing effect to the rough surface micro-uniformities of the polymer matrix, thereby contributing to the creation of a more uniform surface texture and structure.

The wettability observed over 15 min further validates the AFM results (Table 1). Among all samples, the PCL:PU/AuNPs scaffold exhibited the greatest improvement in wettability, as evidenced by a significant drop in the contact angle to 47° after 15 min. This improvement is related to the synergistic effect of the smooth surface topography (Ra = 262 nm) and the presence of AuNPs, which have a beneficial effect on the spreading and penetration of liquids, without the presence of air pockets, an effect in perfect accordance with the Wenzel wetting model. This shift from a hydrophobic surface to a hydrophilic one is clearly at the 15 min mark and provides a promising surface for further protein binding and cell integration, fulfilling the need for a stable, bioactive

surface for tissue engineering.

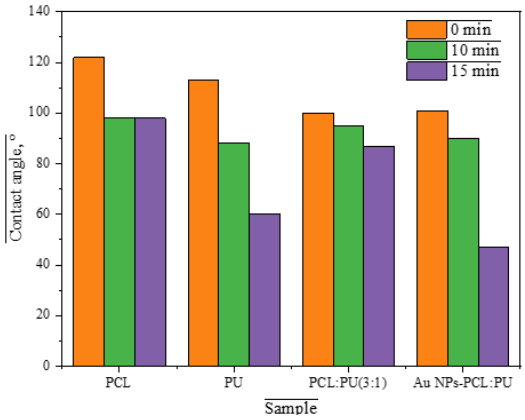

Figure 8. Water contact angle (WCA) results of electrospun scaffolds with different compositions

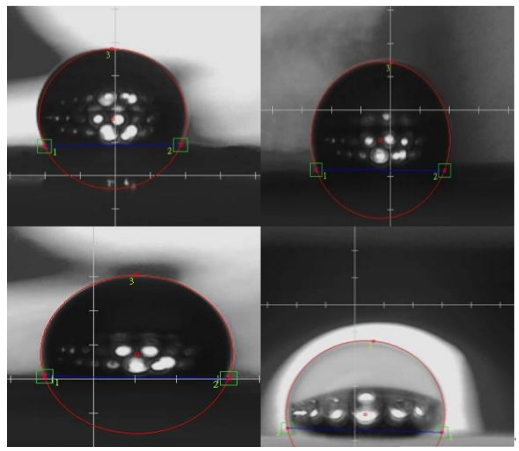

Figure 9. Water contact angle (WCA) images of electrospun scaffolds with different compositions at 0 min

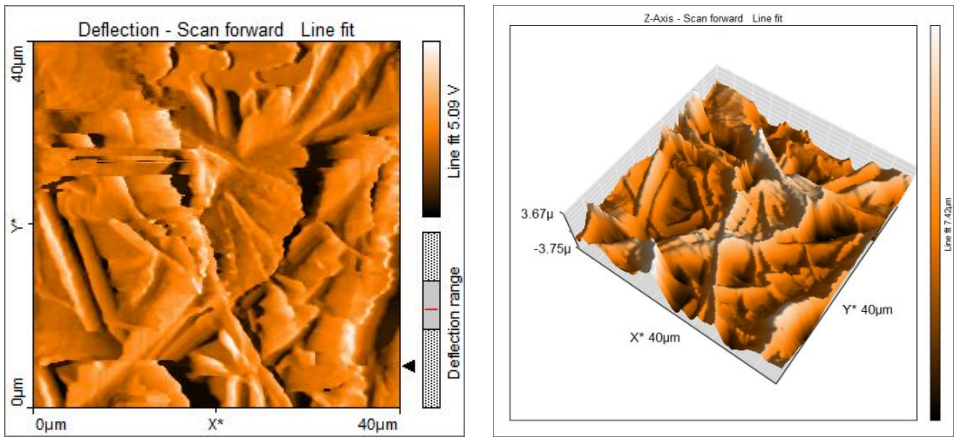

(A)

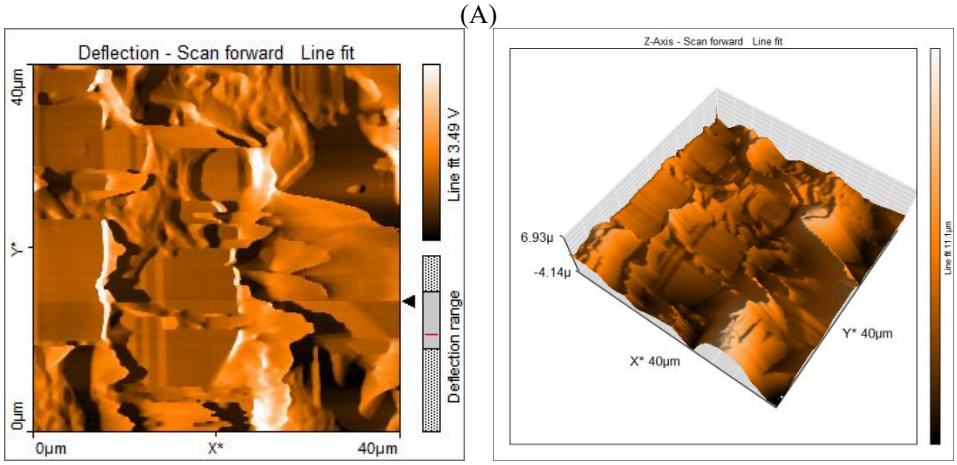

(B)

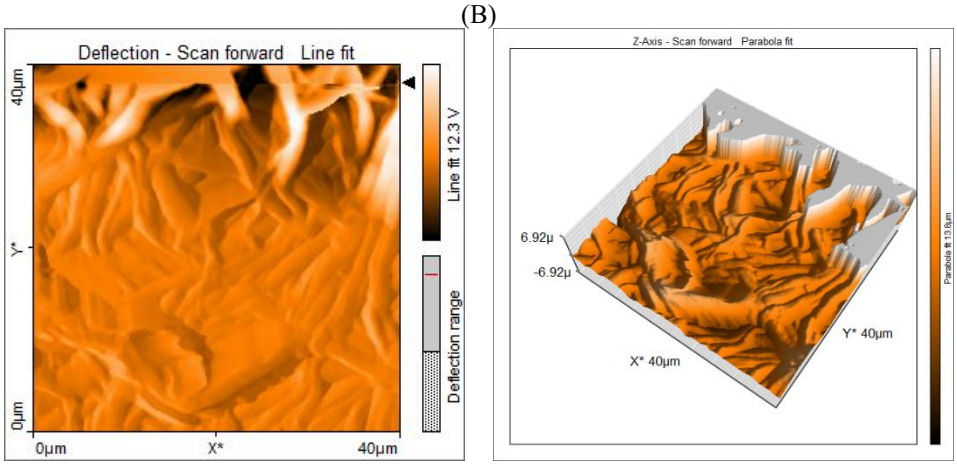

(C)

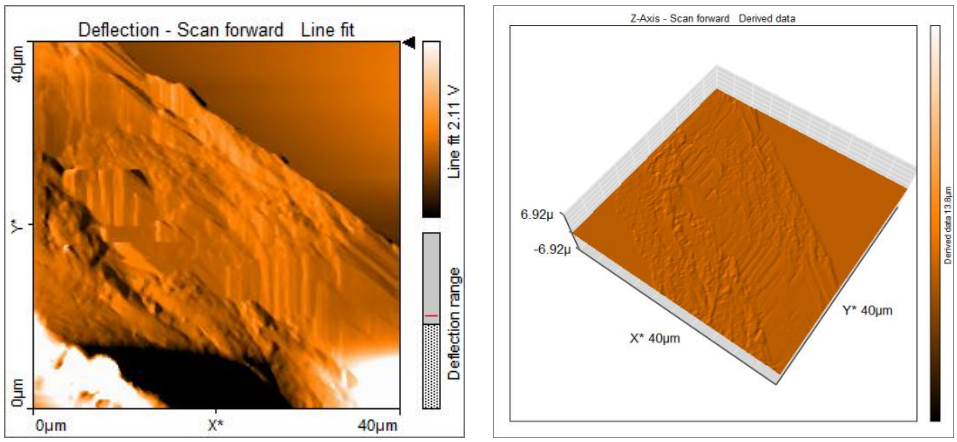

(D)

Figure 10. Atomic force microscopy (AFM) analysis of the electrospun nanofibers: (A) polycaprolactone (PCL), (B) polyurethane (PU), (C) PCL:PU and PCL:PU-loaded gold nanoparticles (AuNPs)

Note: The 2D topographical image and 3D surface representations of the fabricated scaffolds. The scan area for samples is 40 × 40 µm^2.

Table 1. Surface roughness (Ra) and water contact angle (WCA)

Sample	Ra (nm)	WCA (0 min)	WCA (10 min)	WCA (15 min)
PCL	1017	121.8°	98°	98°
PU	1035	113°	88°	60°
PCL:PU	555	100°	95°	87°
PCL:PU-AuNPs	262	101°	90°	47°

Note: Polycaprolactone (PCL), polyurethane (PU), gold nanoparticles (AuNPs).

4. CONCLUSION

In this study, we successfully developed and characterized electrospun PCL:PU structures decorated with AuNPs. Blending PU with PCL effectively increased fiber diameter and pore size, which likely facilitates nutrient diffusion and cell infiltration. FTIR analysis verified the successful physical blending process, suggesting that interaction between AuNPs and the polymer matrix occurs at the surface level. The structures could be improved with the incorporation of AuNPs, enhancing the electrical conductivity and providing an appropriate conductive surface at which to study electrically responsive tissues. Moreover, surface wettability studies have revealed that the wettability of the surface can be controlled by the structural composition. Overall, the PCL:PU-AuNPs structures have good structural and electrical properties. These findings show that it has the potential to be a platform for cardiac tissue engineering; however, further study of its mechanical properties and biological interactions is warranted to substantiate its use in clinical applications for cardiology.

REFERENCES

[1] Mozaffarian, D., Benjamin, E.J., Go, A.S., et al. (2016). Heart disease and stroke statistics—2016 update: A report from the American Heart Association. Circulation, 133(4): e38-e360. https://doi.org/10.1161/cir.0000000000000350

[2] Zimmermann, W.H., Schneiderbanger, K., Schubert, P., et al. (2002). Tissue engineering of a differentiated cardiac muscle construct. Circulation Research, 90(2): 223-230. https://doi.org/10.1161/hh0202.103644

[3] Bursac, N., Papadaki, M., Cohen, R.J., et al. (1999). Cardiac muscle tissue engineering: Toward an in vitro model for electrophysiological studies. American Journal of Physiology-Heart and Circulatory Physiology, 277(2): H433-H444. https://doi.org/10.1152/ajpheart.1999.277.2.h433

[4] Acharya, R., Dutta, S.D., Patil, T.V., Ganguly, K., Randhawa, A., Lim, K.T. (2023). A review on electroactive polymer–metal composites: Development and applications for tissue regeneration. Journal of Functional Biomaterials, 14(10): 523. https://doi.org/10.3390/jfb14100523

[5] Khademhosseini, A., Langer, R., Borenstein, J., Vacanti, J.P. (2006). Microscale technologies for tissue engineering and biology. Proceedings of the National Academy of Sciences of the United States of America, 103(8): 2480-2487. https://doi.org/10.1073/pnas.0507681102

[6] Balint, R., Cassidy, N.J., Cartmell, S.H. (2014). Conductive polymers: Towards a smart biomaterial for tissue engineering. Acta Biomaterialia, 10(6): 2341-2353. https://doi.org/10.1016/j.actbio.2014.02.015

[7] Mohaddesi, M., Jahani, A., Vahedi, E., et al. (2024). Creating and evaluating a novel small diameter PCL/PU vascular graft for finger reconstruction: A comprehensive analysis of structural, mechanical, in vitro, and in vivo assessments. Materials Today Communications, 40: 109427. https://doi.org/10.1016/j.mtcomm.2024.109427

[8] Woodruff, M.A., Hutmacher, D.W. (2010). The return of a forgotten polymer—Polycaprolactone in the 21st century. Progress in Polymer Science, 35(10): 1217-1256. https://doi.org/10.1016/j.progpolymsci.2010.04.002

[9] Nguyen, T.H., Padalhin, A.R., Seo, H.S., Lee, B.T. (2013). A hybrid electrospun PU/PCL scaffold satisfied the requirements of blood vessel prosthesis in terms of mechanical properties, pore size, and biocompatibility. Journal of Biomaterials Science, Polymer Edition, 24(14): 1692-1706. https://doi.org/10.1080/09205063.2013.792642

[10] Nazari, H., Azadi, S., Hatamie, S., et al. (2019). Fabrication of graphene-silver/polyurethane nanofibrous

scaffolds for cardiac tissue engineering. Polymers for Advanced Technologies, 30(8): 2086-2099. https://doi.org/10.1002/pat.4641
[11] Dykman, L., Khlebtsov, N. (2012). Gold nanoparticles in biomedical applications: Recent advances and perspectives. Chemical Society Reviews, 41(6): 2256-2282. https://doi.org/10.1039/c1cs15166e
[12] Huang, X., Jain, P.K., El-Sayed, I.H., El-Sayed, M.A. (2007). Gold nanoparticles: Interesting optical properties and recent applications in cancer diagnostics and therapy. Nanomedicine, 2(5): 681-693. https://doi.org/10.2217/17435889.2.5.681
[13] Li, D., Xia, Y. (2004). Electrospinning of nanofibers: Reinventing the wheel? Advanced Materials, 16(14): 1151-1170. https://doi.org/10.1002/adma.200400719
[14] Fleischer, S., Shevach, M., Feiner, R., Dvir, T. (2014). Coiled fiber scaffolds embedded with gold nanoparticles improve the performance of engineered cardiac tissues. Nanoscale, 6(16): 9410-9414. https://doi.org/10.1039/c4nr00300d
[15] Qin, X., Wu, D. (2012). Effect of different solvents on poly(caprolactone) (PCL) electrospun nonwoven membranes. Journal of Thermal Analysis and Calorimetry, 107(3): 1007-1013. https://doi.org/10.1007/s10973-011-1640-4
[16] Mousavi, A., Vahdat, S., Baheiraei, N., Razavi, M., Norahan, M.H., Baharvand, H. (2021). Multifunctional conductive biomaterials as promising platforms for cardiac tissue engineering. ACS Biomaterials Science & Engineering, 7(1): 55-82. https://doi.org/10.1021/acsbiomaterials.0c01422
[17] Azine, Z., Moeini, M., Solouk, A., Akbari, S. (2023). Polyurethane-calcium peroxide composite nanofibrous scaffolds with controlled oxygen release for tissue engineering applications. Nano, 18(02). https://doi.org/10.1142/s1793292023500121
[18] Abdelrazek, E.M., Hezma, A.M., El-khodary, A., Elzayat, A.M. (2016). Spectroscopic studies and thermal properties of PCL/PMMA biopolymer blend. Egyptian Journal of Basic and Applied Sciences, 3(1): 10-15. https://doi.org/10.1016/j.ejbas.2015.06.001
[19] Pooshidani, Y., Zoghi, N., Rajabi, M., Haghbin Nazarpak, M., Hassannejad, Z. (2021). Fabrication and evaluation of porous and conductive nanofibrous scaffolds for nerve tissue engineering. Journal of Materials Science: Materials in Medicine, 32: 46. https://doi.org/10.1007/s10856-021-06519-5
[20] Ming, G., Henley, J., Tessier-Lavigne, M., Song, H., Poo, M. (2001). Electrical activity modulates growth cone guidance by diffusible factors. Neuron, 29(2): 441-452. https://doi.org/10.1016/s0896-6273(01)00217-3
[21] Vogt, L., Boccaccini, A.R. (2021). Random and aligned electrospun poly(ε-caprolactone) (PCL)/poly(1, 8-octanediol-co-citrate) (POC) fiber mats for cardiac tissue engineering using benign solvents. European Polymer Journal, 160: 110772. https://doi.org/10.1016/j.eurpolymj.2021.110772
[22] Ghasemi-Mobarakeh, L., Prabhakaran, M.P., Morshed, M., et al. (2011). Application of conductive polymers, scaffolds and electrical stimulation for nerve tissue engineering. Journal of Tissue Engineering and Regenerative Medicine, 5(4): e17-e35. https://doi.org/10.1002/term.383
[23] Vial, S., Reis, R.L., Oliveira, J.M. (2017). Recent advances using gold nanoparticles as a promising multimodal tool for tissue engineering and regenerative medicine. Current Opinion in Solid State and Materials Science, 21(2): 92-112. https://doi.org/10.1016/j.cossms.2016.03.006
[24] Wu, J.C.C., Ray, S., Gizdavic-Nikolaidis, M., et al. (2014). Nanostructured bioactive material based on polycaprolactone and polyaniline fiber-scaffolds. Synthetic Metals, 198: 41-50. https://doi.org/10.1016/j.synthmet.2014.09.017
[25] Cassie, A.B.D., Baxter, S. (1944). Wettability of porous surfaces. Transactions of the Faraday Society, 40: 546. https://doi.org/10.1039/tf9444000546
[26] Zamani, F., Amani-Tehran, M., Latifi, M., Shokrgozar, M.A. (2013). The influence of surface nanoroughness of electrospun PLGA nanofibrous scaffold on nerve cell adhesion and proliferation. Journal of Materials Science: Materials in Medicine, 24(6): 1551-1560. https://doi.org/10.1007/s10856-013-4905-6
[27] Diego, R.B., Olmedilla, M.P., Aroca, Á.S., et al. (2005). Acrylic scaffolds with interconnected spherical pores and controlled hydrophilicity for tissue engineering. Journal of Materials Science, 40(18): 4881-4887. https://doi.org/10.1007/s10853-005-3885-4
[28] Stuart, B.H. (2004). Infrared Spectroscopy: Fundamentals and Applications, 1st ed. John Wiley & Sons.

NOMENCLATURE

Da	Daltons
PCL	polycaprolactone
PU	polyurethane
Mw	molecular weight
SEM	scanning electron microscopy
FTIR	Fourier transform infrared spectroscopy
AuNPs	gold nanoparticles
CVDs	cardiovascular diseases
CNTs	carbon nanotubes
ECM	native extracellular matrix
DCM	Dichloromethane
DMF	N,N-dimethylformamide
kV	kilovolta
cm	centimeter
mL	milliliter
h	hour
EDS	energy dispersive X-ray spectroscopy
WCA	water contact angle
AFM	atomic force microscopy
nm	nanometer
R	electrical resistance
L	length
W	width
t	thickness
Ra	surface roughness
Rq	root-mean-square roughness

Greek symbols

ρ	resistivity
σ	electrical conductivity, S/cm
μm	micrometer